Three-dimensional dynamics of detonation diffraction: effects of the tube cross-section shape

V. Monnier, V. Rodriguez, P. Vidal, R. Zitoun

Institut Pprime, UPR 3346, ENSMA, BP 40109, 86961 Futuroscope-Chasseneuil, France

1. Introduction

In a previous study [1, 2], we investigated the conditions under which the cross-section shape of a tube influences the cellular structure of a detonation steadily propagating in this tube. The present experimental work reports on the influence of the cross-section shape on the transient phenomena observed after a steady detonation diffracts through a single-orifice plate positioned normally to the longitudinal axis of the tube.

The interaction of detonation and deflagration with perforated obstacles has been the object of a large amount of work. Ciccarelli carried out a comprehensive review [3]. The topic is relevant to safety in industrial plants, detonation enhancement or mitigation, e.g., [4]. Obstacles and perforated plates in tubes can either enhance flame acceleration and deflagration-to-detonation transition (DDT) [5], or quench detonations. Parametric studies include the effects of the blockage ratio, the spacing and the number of the orifices, e.g., [6], the shape of the orifices, e.g., [7], the equivalence ratio and the initial pressure and temperature of the mixture, e.g., [8], the regularity of the detonation cells.

To our knowledge, the cross-section shapes of the tube and the orifice in a perforated plate have yet to be investigated, which is the object of the present work. Section 2 presents the experimental setup and the methodology, section 3 the results, and Section 4 the discussion.
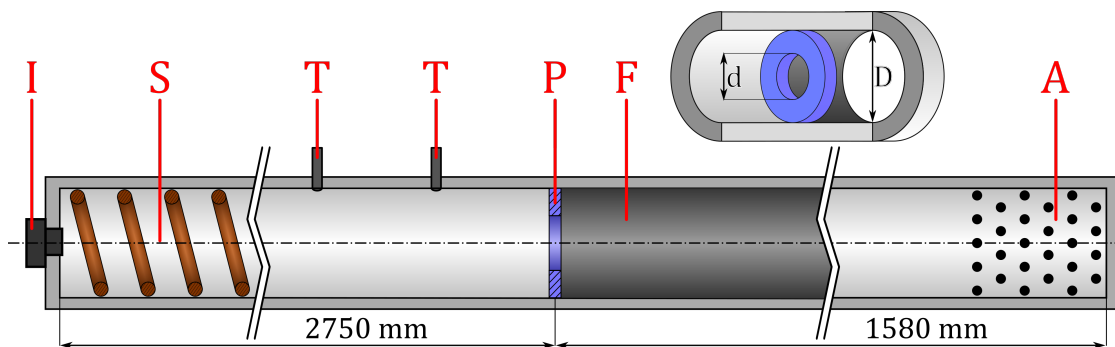
2. Setups and methodology

Figure 1: Schematic of the round tube (that of the square tube is similar). I: ignition device, S: Shchelkin spiral, T: pressure transducers, P: perforated plate, F: soot foil, A: shock absorber.

We carried out the experiments in tubes with different cross-section shapes, namely round or square, but with the same cross-section area $1600 \pm 4\%$ mm². We chose the same shape of the orifice in the plate as the tube cross-section, e.g., Fig.1. We defined the blockage ratio as the obstructed area of the plate relative to that of the tube cross-section, that is BR$= 1 - (d/D)^2$ for the round tube, with d and D the diameters of the orifice and the tube, and BR$= 1 - (a/a_t)^2$ for the square tube, with a and a_t the widths of the orifice

and the tube. We considered the three values BR= 25, 50 and 75%. All plates have the same thickness of 5 mm.

We used a spark plug or an exploding wire for ignition, depending on p_0, and a 700 mm long Shchelkin spiral to ensure a rapid transition to detonation. The perforated plate was located 2750 mm ahead of the ignition, and previous works [1, 2] showed the detonation has become steady at that distance.

We positioned soot-coated foils along the tube walls downstream of the plate to obtain longitudinal soot recordings of the diffraction processes. In the square tube, we also positioned a foil upstream of the plate to record the cellular structure of the detonation before its diffraction. All foils were 30 cm long.

We carried out chemiluminescence and shadowgraph recordings in the square tube after substituting quartz windows for facing metallic walls. We positioned Kistler 603B pressure transducers coupled with Kistler 5018A electrostatic charge amplifiers upstream of the plate. We used their signals to trigger the high-speed visualizations - and, additionally, to check the detonation steadiness and velocity. We chose the offset depending on the detonation velocity. We implemented an HPVX-2 camera with a frequency ranging from 1 to 5 MHz depending on the detonation velocity. The exposure time was between 200 and 500 ns for shadowgraph imaging and about 600 ns for chemiluminescence. We set the camera to detect a large-spectrum chemiluminescence from the combustion process and its products. We could not implement chemiluminescence for $p_0 \leq 30.0$ kPa because the emission signals had too weak magnitudes.

We positioned a ball of iron wool at the tube ends opposite the ignition. Its object was used to absorb shocks and prevent possible re-ignition of the unburnt mixture in the cases where detonation failed to re-ignite downstream of the obstacle.

The reactive gases were the stoichiometric mixtures $2\,H_2 + O_2$ and $2\,H_2 + O_2 + 2\,Ar$. They were prepared in a separate tank using the partial-pressure method and then injected at the desired initial pressure p_0 after vacuuming the tubes. The initial temperature was 294 ± 3 K, and p_0 varied from 7.5 to 80.0 kPa.

3.   Results

The table in Figure 2 summarizes the diffraction phenomena downstream of the obstacle for each considered cross-section shapes, blockage ratio BRs, mixture compositions, and initial pressures p_0. The analysis evidences a major effect of the cross-section shape on the phenomenology of the detonation diffraction, regardless of the other parameters. We observed five diffraction types, namely:

- F: Failure of detonation transmission.
- DDT: Deflagration-to-Detonation Transition,
- SSO: Shock-Shock Onset,
- CO: Onset at the corners of the square tube,
- SWO: Shock-Wall Onset,

With increasing p_0, the re-initiation mechanisms in the round tube are DDT, SSO and SWO and, in the square tube, SSO, CO and SWO. Their common feature is that the diffraction, downstream of the plate, produces a diverging shock that first decouples from the combustion wave and then reflects at the tube walls. The mechanisms distinguish from each other depending on the events after this reflection.

The DDT mechanism, e.g., Fig. 3b, is observed only in the round tube with the transition position varying from one experiment to another, probably because of its high sensitivity to defects at walls. The usual DDT process observed in tubes with large enough transverse dimensions comprises flame acceleration, shock formation ahead of the flame, explosion between the flame and the shock, and relaxation into a self-sustained detonation.

2H₂+O₂+2Ar, BR=75%

	7.5	12.5	15.0	17.5	40.0	50.0	60.0
□ (square)	F	F	SSO	CO	CO	CO & SWO	SWO
○ (round)	F				F	DDT	SWO

2H₂+O₂, BR=75%

	12.5	15.0	17.5	20.0	30.0	40.0	60.0	70.0	80.0
□ (square)	F	SSO	CO				CO	CO & SWO	SWO
○ (round)	F				F	DDT	SSO	SSO	SWO

2H₂+O₂+2Ar, BR=50%

	10.0	12.5	15.0	17.5	20.0	40.0	50.0
□ (square)	SSO	SSO	CO & SSO	CO & SSO	CO & SWO	CO & SWO	SWO
○ (round)	SSO		SSO	SWO			SWO

2H₂+O₂, BR=50%

	10.0	17.5	20.0	40.0	50.0
□ (square)	SSO	SSO	CO & SWO	CO & SWO	SWO
○ (round)	SSO	SWO			SWO

2H₂+O₂+2Ar, BR=25%

	7.5
□ (square)	Transmission
○ (round)	Transmission

2H₂+O₂, BR=25%

	7.5	10.0
□ (square)	SSO	Transmission
○ (round)	Transmission	

Figure 2: Summary of the diffraction behaviors after the detonation passes through the orifice plate depending on the cross-section shape of the tube, blockage ratio BR, Argon dilution and initial pressure p_0. F: detonation failure, SSO: Shock-Shock Onset, CO: Corner Onset, SWO: Shock-Wall Onset, DDT: Deflagration-to-Detonation Transition.

The SSO mechanism, e.g., Fig. 3c and Fig. 3f, is detonation re-initiation at the tube axis resulting from the focus of a converging shock originating from the tube wall(s). The reflection of the diverging shock at the wall(s) produces Mach stems and a shock converging symmetrically towards the centre of the cross-section. Its focus ignites a local explosion on the tube axis that eventually relaxes into a steady detonation. There is no re-ignition at the wall(s) behind the Mach stems. The re-ignited detonation is first non-ideal because its cell widths are first larger than for the self-sustained detonation, before decreasing to values identical to those downstream of the plate. The non-ideal cellular structure with Argon dilution immediately after the shock focus is more irregular than upstream of the obstacle.

The CO mechanism, e.g., Fig. 3d and Fig. 4, is detonation re-initiation at the corners of the square tube. Each Mach stem produced by the reflection of the diffracted shock at a wall interacts with the other propagating towards the same corner line along the adjacent wall. This interaction results in an overdriven detonation, as its cells are smaller in the volume shocked by the Mach stems. This overdriven detonation propagates in all directions in the shocked domain before relaxing into the self-sustained regime. The re-initiation points are located at a shorter distance to the obstacle than the focus point of the converging shock in the SSO mechanism.

The SWO mechanism, e.g., Fig. 3e and Fig. 4, is immediate detonation re-initiation at the impact locations of the diffracted shock with the tube wall(s). In contrast to the CO mechanism, the Mach stem is strong enough to immediately re-ignite the reactive mixture. The resulting explosion is an overdriven detonation - because of its small cells - that eventually relaxes into the self-sustained detonation. The diffracted shock shows a symmetrically-curved surface, regardless of the cross-section shape of the tube. The contact set with the wall of the round tube is a circumferential line. The contact set with the walls of the square tube comprises four points, each located on the centre line of each wall, at mid-distance from its corner lines.

We found that the re-initiation distances for SSO, CO, and SWO depend only on the cross-section shape and BR, without observable effects of p_0 or the Argon-dilution, in the considered ranges of their variations. Indeed, the soot plates and the shadowgraph images show diffracted waves and reflected shocks that follow roughly the same path regardless of p_0 or the Argon dilution. In the square tube, we observed smooth SSO-

CO and CO-SWO transitions with increasing p_0 for each chosen BR and Argon dilution. That explains why soot traces are sometimes asymmetrical when the CO mechanism occurs at one pair of facing walls and the SWO mechanism at the other. We speculate that only the DDT and SSO processes coexist in the round tube if the DDT run-up distance is short enough.

Regardless of the diffraction type, the limiting initial pressure p_0 separating detonation failure from transmission depends on the cross-section shape of the tube, depending on the mixture and BR. For example, the limiting p_0 is between 12.5 and 15.0 kPa in the square tube, and $p_0 = 40.0$ and 50.0 kPa in the round one for BR= 75% and the Argon-diluted mixture, e.g., 3b.

4.   Discussion

The results above show that the cross-section shape of the tube has a strong influence on the transients mechanisms of detonation diffraction through an orifice with the same cross-section shape as the tube. Five diffraction types are identified, namely F, DDT, SSO, CO and SWO. Given the mixture and BR, this influence manifests itself both by the nature of the detonation re-initiation mechanisms and the ranges of initial pressures for observing one or another mechanism.

Overall, detonation transmission in the square tube is achieved with a lower p_0 than in the round tube, other parameters being equal. In our former work [1, 2], we showed that the cross-section shape of the tube influences the cell widths and patterns below a limiting initial pressure p_0, with smaller cells in the square tube. Therefore, the present results are coherent with the former because their respective ranges of p_0 partly coincide with each other. Nevertheless, whether the diffraction mechanism is independent of the tube cross-section shape with p_0 sufficiently large, and whether the diffraction behaviours and the cell patterns of the steady detonation are independent of this shape for the same limiting p_0, have yet to be investigated.

References

[1] V. Monnier, V. Rodriguez, P. Vidal, R. Zitoun, Experimental analysis of cellular detonations: a discussion on regularity and three-dimensional patterns, oral presentation # 57 to the 28th ICDERS, Naples (2022)

[2] V. Monnier, V. Rodriguez, P. Vidal, R. Zitoun, An analysis of three-dimensional patterns of experimental detonation cells, Combustion and Flame, 245 (2022) 112310 | doi:10.1016/j.combustflame.2022.112310

[3] G. Ciccarelli, S. Dorofeev, Flame acceleration and transition to detonation in ducts, Progress in Energy and Combustion Science, 34 (2008) 499-550 | doi:10.1016/j.pecs.2007.11.002

[4] B. Zhang, H. Liu, The effects of large scale perturbation-generating obstacles on the propagation of detonation filled with methane–oxygen mixture, Combustion and Flame, 182 (2017) 279-287 | doi:10.1016/j.combustflame.2017.04.025

[5] G.B. Goodwin, R.W. Houim, E.S. Oran, Effect of decreasing blockage ratio on DDT in small channels with obstacles, Combustion and Flame, 173 (2016) 16-26 | doi:10.1016/j.combustflame.2016.07.029

[6] V. Rodriguez, V. Monnier, P. Vidal, R. Zitoun, Towards non-dimensionalized distances and limits for transition of deflagration to detonation, Shock Waves, 32 (2022) 417-425, | doi:10.1007/s00193-022-01088-0

[7] L.Q. Wang, H.H. Ma, Z.W. Shen, M.J. Lin, X.J. Li, Experimental study of detonation propagation in a square tube filled with orifice plates, International Journal of Hydrogen Energy, 43 (2018) 4645-4656 | doi:10.1016/j.ijhydene.2018.01.080

[8] G. Ciccarelli, J.L. Boccio, Detonation wave propagation through a single orifice plate in a circular tube, Symposium (International) on Combustion, 27 (1998) 2233-2239 | doi:10.1016/S0082-0784(98)80072-6
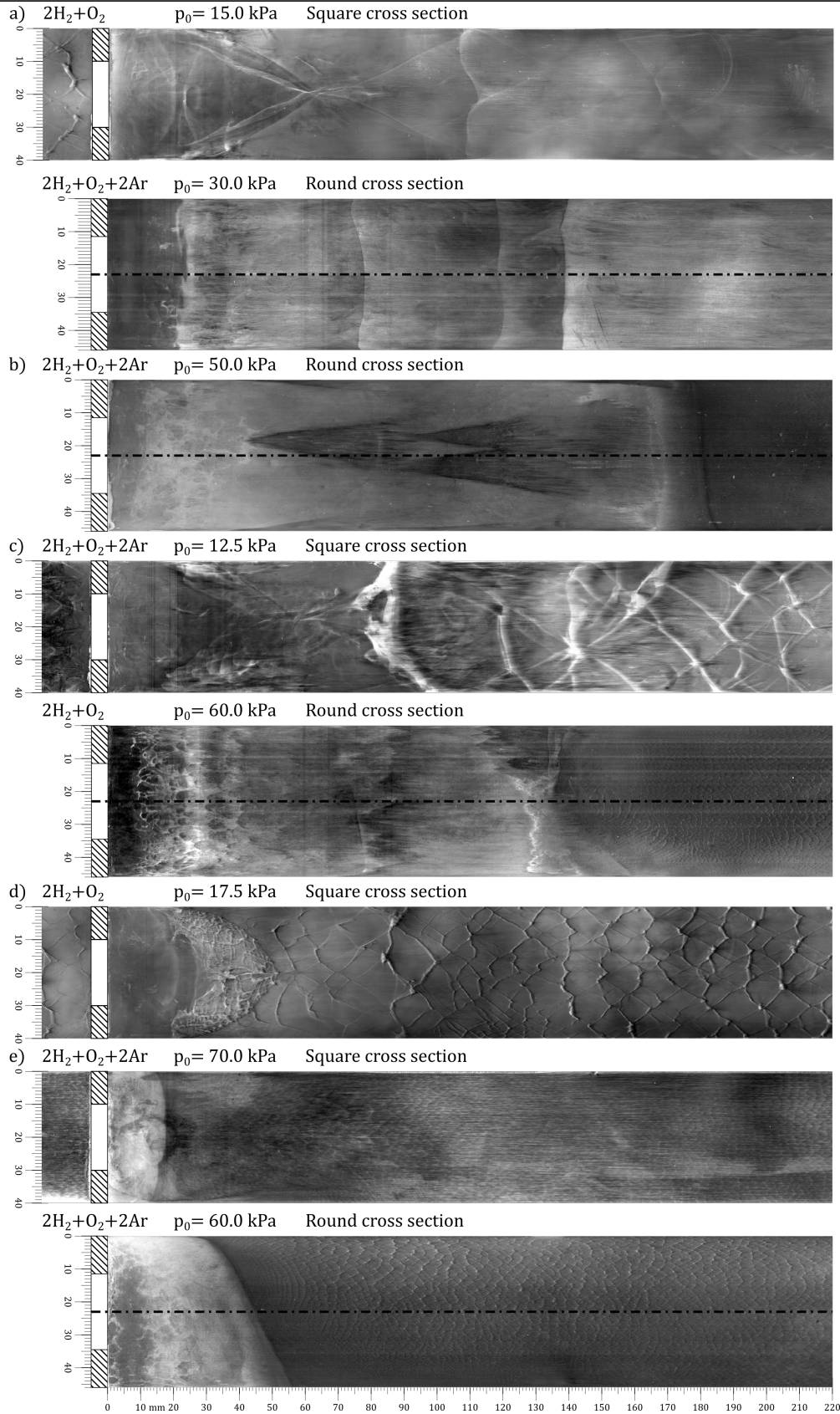
Figure 3: Examples of soot recordings obtained in the square (left) and round (right) cross-section tubes for BR= 75% and tube cross-section area $1600 \pm 4\%$ mm^2. a: Detonation failure, b: SSO mechanism, c: DDT mechanism, d: CO mechanism, e: SWO mechanism.
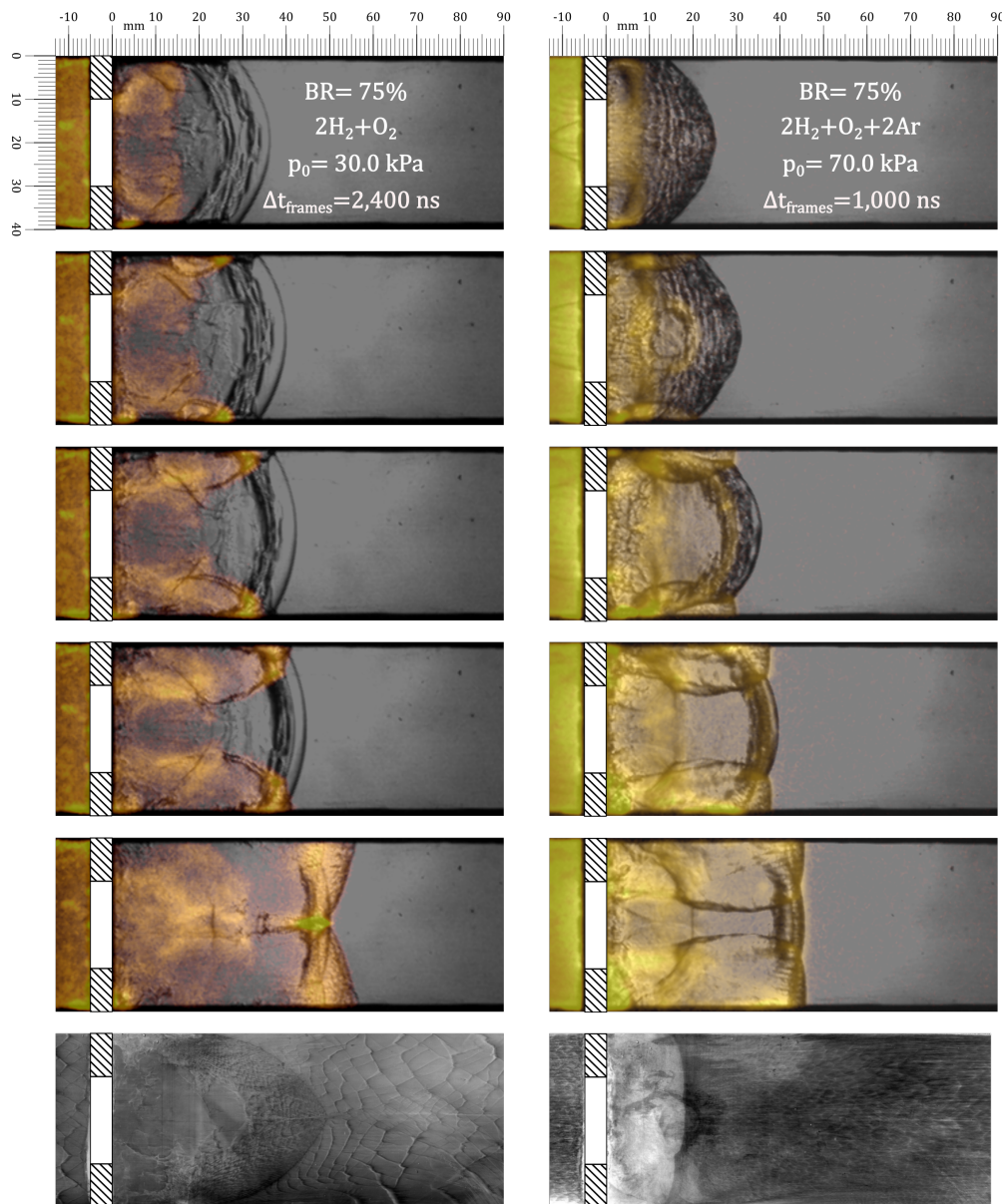
Figure 4: Superimposed shadowgraph and chemiluminescence images of CO (left) and SWO (right) mechanisms in the square tube, with corresponding soot recordings (bottom).